A 27 kyr terrestrial biomarker record in the southern Indian Ocean

Marie-Alexandrine Sicre, Laurent Labeyrie, Ullah Ezat, Alain Mazaud, Jean-Louis Turon

Geochemistry Geophysics Geosystems G3
AN ELECTRONIC JOURNAL OF THE EARTH SCIENCES
Published by AGU and the Geochemical Society

Research Letter
Volume 7, Number 7
28 July 2006
Q07014, doi:10.1029/2005GC001234
ISSN: 1525-2027

A 27 kyr terrestrial biomarker record in the southern Indian Ocean

Marie-Alexandrine Sicre, Laurent Labeyrie, Ullah Ezat, and Alain Mazaud
Laboratoire des Sciences du Climat et de l'Environnement, LSCE-IPSL UMR 1572, Domaine du CNRS, Avenue de la Terrasse, F-91198 Gif-sur-Yvette, France (marie-alexandrine.sicre@lsce.cnrs-gif.fr)

Jean-Louis Turon
Département de Géologie et Océanographie, UMR CNRS 5805, Université de Bordeaux I, 1 Avenue des Facultés, F-33405 Talence Cedex, France

[1] Terrestrial inputs were reconstructed using high molecular weight *n*-alkane concentrations recorded in the sub-Antarctic Indian Ocean core MD94-103 (45°35′S, 86°31′E, 3560 m) to examine regional changes in the atmospheric circulation over the last 27 kyr. This record was compared to the dust content of EPICA-Dome C ice and continental data from South Africa (e.g., pollen sequences and isotope records in speleothems) to get a comprehensive understanding of atmospheric links between low and midlatitudes of the Indian Ocean. Terrestrial *n*-alkanes indicate higher glacial than Holocene inputs and marked glacial oscillations. Minimum values during the Last Glacial Maximum (LGM) are consistent with colder and drier climate and presumably caused by the persistence of subtropical anticyclones over southern Africa limiting the amount of rainfall and vegetation growth. The otherwise higher glacial *n*-alkanes suggest a stronger influence of the tropical rainfall in southern Africa, likely associated with a contraction of the polar vortex with respect to its LGM position. During northern Heinrich events, moderate decline of *n*-alkanes suggests reduced rainfall over southern Africa possibly caused by weaker tropical easterly winds when, according to Stott et al. (2002), the Pacific Ocean would have experienced Super-ENSO conditions.

Components: 5185 words, 3 figures.

Keywords: biomarker; glacial; Indian Ocean; marine sediments; paleoclimate; terrestrial.

Index Terms: 3344 Atmospheric Processes: Paleoclimatology (0473, 4900); 4924 Paleoceanography: Geochemical tracers; 4926 Paleoceanography: Glacial.

Received 29 December 2005; **Revised** 25 April 2006; **Accepted** 11 May 2006; **Published** 28 July 2006.

Sicre, M.-A., L. Labeyrie, U. Ezat, A. Mazaud, and J.-L. Turon (2006), A 27 kyr terrestrial biomarker record in the southern Indian Ocean, *Geochem. Geophys. Geosyst.*, *7*, Q07014, doi:10.1029/2005GC001234.

1. Introduction

[2] The Indian Ocean is an important element of the global heat and hydrological budget. Tropical heat accumulated in Indian Ocean surface waters is vented in the atmosphere and transported to higher latitudes. Meridional heat transfer also occurs through the Agulhas Current, a major conduit of warm waters linking the tropical Indian Ocean to midlatitudes of the southern Indian Ocean [*Quartly and Srokosz*, 1993; *Rintoul et al.*, 2001]. Although, the Indian Ocean is part of the global ENSO (El Niño-Southern Oscillation) teleconnection, the exact links between the Indian and Pacific Ocean

climate are not fully understood [*Saji et al.*, 1999; *Webster et al.*, 1999]. However, it has been observed that ENSO warm events in the equatorial Pacific and Indian Oceans are associated with dry conditions over southern Africa and wet conditions over eastern Africa.

[3] The influence of tropical forcing can be studied by investigating remote midlatitude Southern Ocean marine cores. Several high-resolution records have recently been generated in the subantarctic Atlantic [*Charles et al.*, 1996; *Sachs et al.*, 2001; *Sachs and Anderson*, 2003], Pacific [*Lamy et al.*, 2004; *Kaiser et al.*, 2005; *Pahnke and Zahn*, 2005] and Indian Ocean [*Sicre et al.*, 2005]. However, except for the later, the paleoclimate signals obtained from these cores appear to have been mainly influenced by high latitude climate changes. The Indian basin provides the opportunity to explore the extratropical influence that low latitude climate might exert through atmospheric (e.g., ENSO) and oceanic connection (e.g., Agulhas Retroflection and Agulhas Return current).

[4] In this study, we generated a unique record of terrestrial biomarker *n*-alkanes obtained at subcentennial resolution from the midlatitude southern Indian Ocean core (MD94-103) over the last 27 kyr. Odd-carbon numbered high molecular weight n-alkanes are major lipid constituents of higher-plant surface leaf waxes. Their occurrence in hemipelagic and pelagic sediments remote from the continent results from long-range atmospheric transport of aerosols by large-scale winds [*Gagosian and Peltzer*, 1987; *Conte and Weber*, 2002; *Sicre and Peltzer*, 2004]. Similar to pollens, their concentrations in marine sediments are controlled by variations in the wind regime and emission rates from the vegetation. However, in contrast to pollens they can travel large distances and reach remote ocean sites. Aerosol monitoring over three years from Bermuda island has shown that leaf waxes are introduced into the atmosphere mainly by wind ablation off the living vegetation rather than from soil remobilization of detrital waxes during soil deflation [*Conte and Weber*, 2002]. Ablated waxes are then transported by winds mainly as micrometer size particles [*Sicre et al.*, 1987] over a rather short time period, on the order of days, till their deposition to the ocean surface. Aerosols thus integrate vegetation waxes over large continental areas. Wax constituents such as *n*-alkanes (or fatty alcohols and fatty acids) are well-preserved in sediments and therefore their stratigraphic record has been used to investigate atmospheric circulation history and changes of the vegetation production [*Huang et al.*, 2001; *Ternois et al.*, 2000; *Hughen et al.*, 2004]. The terrestrial input record of MD94-103 was compared to dust fallout in Antarctica (EPICA Dome C) and available continental *proxy* records (pollens and speleothems) from South Africa (Figure 1) to infer atmospheric circulation changes during the last glacial period. Sea Surface temperatures (SSTs) determined in exactly the same sediment horizons were used to further discuss ocean-atmosphere interactions.

2. Methodology

2.1. Age Model

[5] The MD94-103 core was retrieved from the subantarctic waters of the Indian sector of the Southern Ocean (45°35′S; 86°31′E, 3560 m water depth) on a protected shoulder of the upper southern slope of the South Indian Ridge, out of reach for long-distance bottom sediment advection [*Sicre et al.*, 2005]. A precise chrono-stratigraphy was developed using paleomagnetic correlation and ^{14}C dates [*Mazaud et al.*, 2002; *Sicre et al.*, 2005]. Briefly, the age scale was derived from the correlation of the relative magnetic field paleointensity of MD94-103 and the NAPIS-75 stack, placed on GISP2 age model. In addition, 10 accelerator mass spectrometry (AMS) ^{14}C dates on 9 sediment horizons, were performed on monospecific foraminifera *G. bulloides* and *N. pachyderma* to determine ages for the upper part of the core. ^{14}C ages were converted to calendar ages using the Calib 4.3 software, the marine calibration Marine 98.14c and a modern local reservoir age of 600 years [*Bard*, 1988]. The depth to age conversion was obtained by linear interpolation between age constrained levels. On the basis of this age scale, sampling resolution is estimated to be less than 50 years in the glacial portion of the record and 100–200 years for the Holocene.

2.2. Biomarker Analyses

[6] Sediments were freeze-dried and grounded in a glass mortar. Lipids were extracted in an ultrasonic bath (10 min), using methylene chloride/methanol (2:1; v/v). Centrifugation was then performed for 10 min at 2000 rpm and the supernatant recovered. These operations, extraction and centrifugation were repeated twice and the three extracts combined to be evaporated to almost dryness using a rotary evaporator. The reduced total extract was

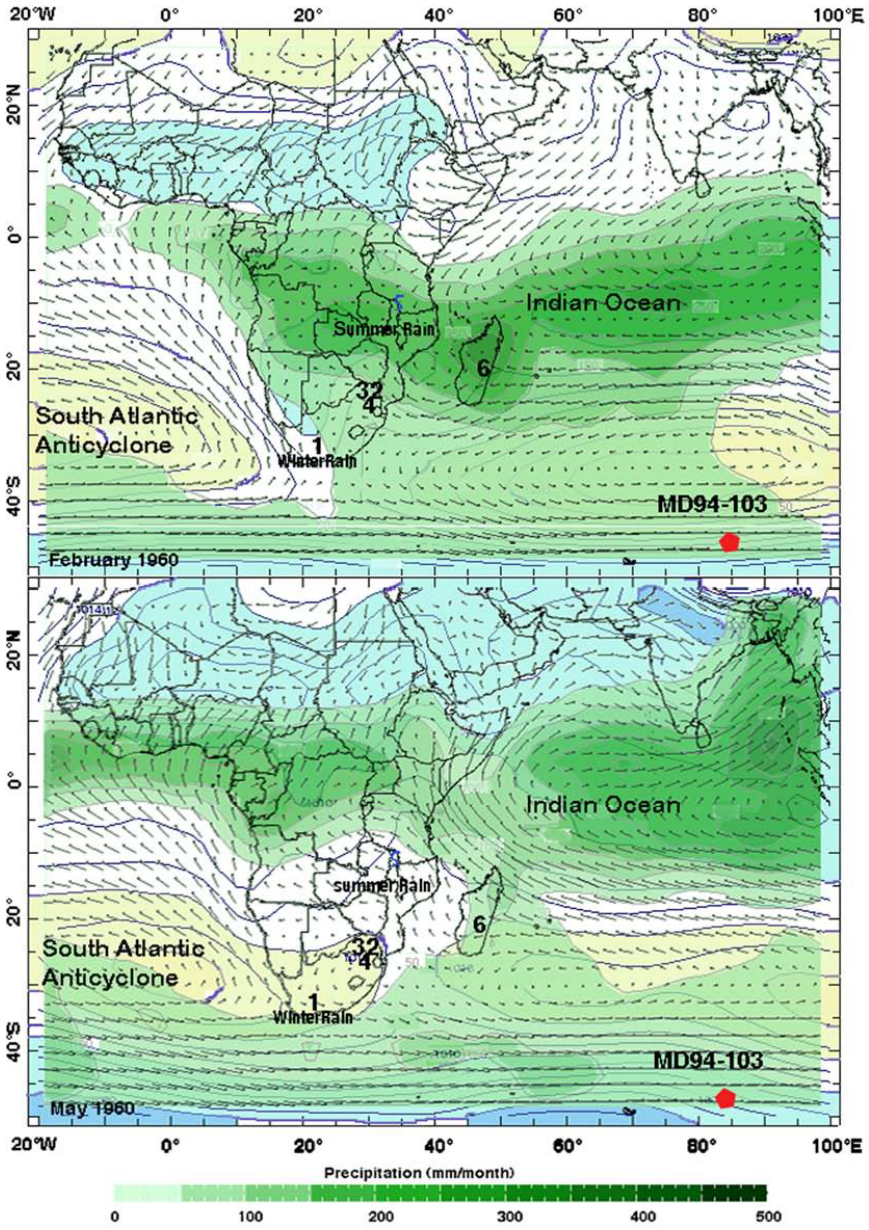

Figure 1. Map of the Southern Hemisphere climatology in the African-Indian ocean sector, for Mean February and Mean May 1960 (plotted from http://iridl.ldeo.columbia.edu/expert/SOURCES/.NOAA/.NCEP-NCAR/). The backward layer gives the pressure distribution at sea level (antycyclonic gyres: dark yellow, above 1020 HPa, light yellow 1020–1016 HPa; cyclonic gyres: light blue 1010–1000 HPa, dark blue less than 1000 HPa). The green overlay gives the mean precipitation distribution (scale as indicated) for the areas over 50 mm/month. Arrows indicate mean winds; their length is proportional to wind intensity. February represents the southern summer climatology, with maximum southern shift of the tropical rain belt. May has been chosen as an approximate analog of the Last Glacial Maximum winter at low latitudes, with the Intertropical Convergence Zone shifted south, and low northern summer monsoon activity, when compared to modern southern winter situation. The expansion of the subtropical anticyclone over South Africa is well apparent (see text). The month of May southern winter analog, however, probably underestimates the northward migration of the westerly belt, and associated depressions, and sea ice at high latitude as reconstructed by *Crosta et al.* [2004]. Plotted are 1, Cango Cave; 2, Makapantsgat Cave; 3, Wonder crater; 4, Tswaing Crater (Pretoria Saltpan); 6, Lake Tritrivakely (Madagascar); and the location of core MD94-103.

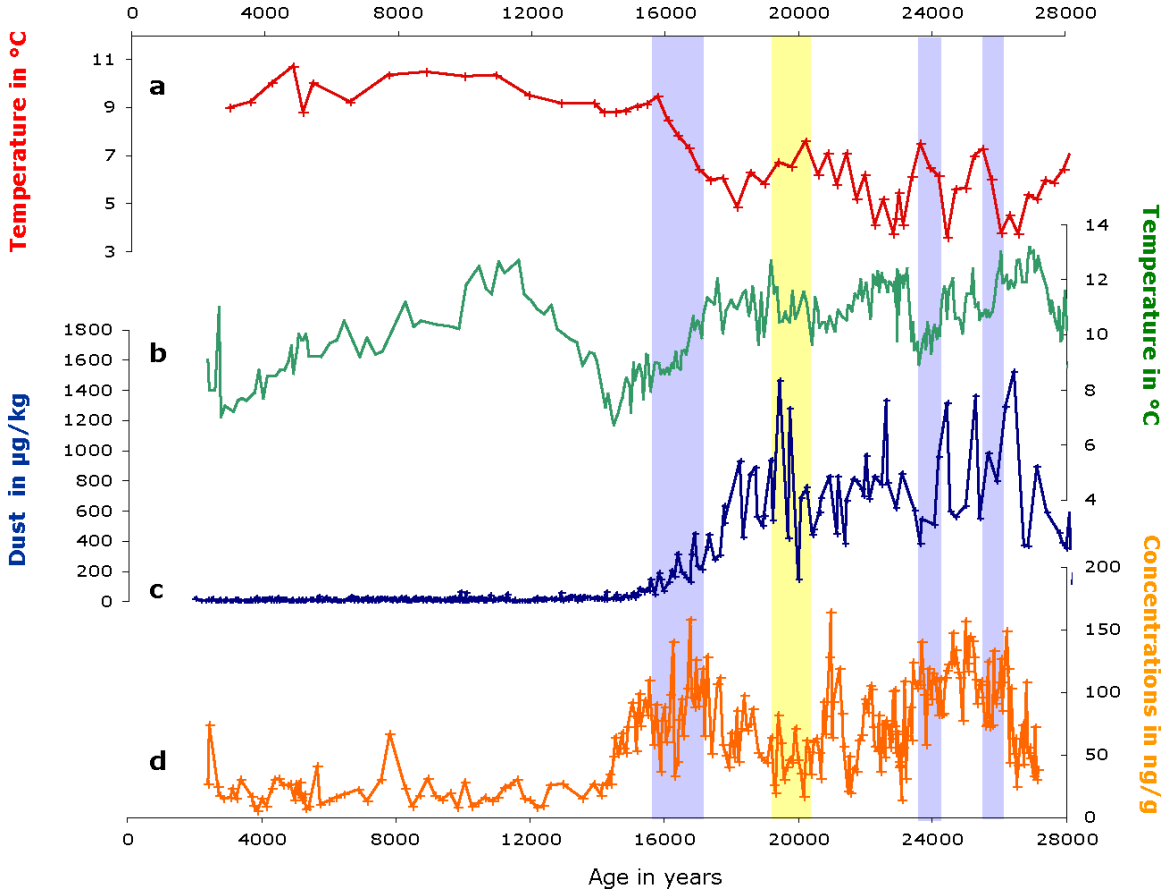

Figure 2. Comparison of the proxy data from the MD94-103 core (45°35′S; 86°31′E, 3560 m) and dust content of EPICA Dome C ice. (a) SST reconstruction based on planktonic foraminifera assemblage (SST_{foram} in the text), using the modern analog technique MAT [from *Sicre et al.*, 2005]. (b) Sea surface temperature obtained using alkenone paleothermometry (SST_{alk} in the text), using the calibration of *Prahl et al.* [1988] [from *Sicre et al.*, 2005]. (c) Dust concentration in µg/kg deposited in EPICA Dome C ice core [from *EPICA Community Members*, 2004]. (d). Sum of the terrestrial biomarkers C27+C29+C31 *n*-alkane concentrations expressed in ng/g determined in the MD94-103 core. Blue vertical bars indicate Heinrich events in the Northern Hemisphere (HE1, HE2a and HE2b). The yellow vertical bar indicates the Last Glacial Maximum.

then transferred to a 4 ml vial and evaporated to dryness under a nitrogen stream. Hydrocarbons were then isolated by silica gel chromatography using 5% deactivated silica gel with pure hexane. They were stored in glass vials at −18°C prior to gas chromatography analyses performed on a Varian CX 3400 series gas chromatograph equipped with a fused CP-Sil-5CB silica capillary column (50 m × 0.32 mm i.d., 0.25 µm film thickness, Chrompack) and a flame ionization detector. The oven temperature was programmed from 100°C to 300°C at 20°C min^{-1}. Helium was used as the carrier gas. Alkenones were analyzed following the procedure described by *Ternois et al.* [1997]. SSTs were calculated from the $U^{K'}_{37}$ index and the calibration published by *Prahl et al.* [1988] ($U^{K'}_{37}$ = 0.034T + 0.039). 5α-cholestane was added prior gas chromatographic injections for *n*-alkane and alkenone quantitation.

3. Results and Discussion

3.1. N-Alkanes Record and EPICA Dust

[7] Figure 2d shows the total concentrations (in ng/g dry weight sediment) of the three odd-carbon numbered high molecular weight homologs (ΣC_{27}-C_{29}-C_{31}) which dominates the *n*-alkane distribution along the core. Values range from about 5 ng g^{-1} to 160 ng g^{-1}, with average glacial levels higher than Holocene ones by about 4 times (21 ± 12 ng g^{-1} versus 79 ± 32 ng g^{-1}). This Holocene/glacial contrast is also observed in the eolian dust record of EPICA-Dome C ice core (75°06′S; 123°21′E) from East Antarctica (Figure 2c) [*EPICA Community*

Members, 2004]. Although both records indicate higher glacial levels, they show differences: (1) The Last Glacial Maximum (LGM) is a period of highest dust in Antarctica but minimum *n*-alkanes deposition in MD94-103. (2) The progressive decline from high dust glacial values occurs ~19 ka in Antarctica ice while *n*-alkanes start to decrease ~17 ka, a 2 kyr offset that cannot be attributed to age models. Yet differences between the two records are not entirely unexpected. Sedimentary *n*-alkanes provide a spatially integrated information of the terrestrial biosphere biomass, whereas mineral dust deposits depend on the extent of arid surfaces. Under dry climate or low precipitation conditions, vegetation growth will be decreased while dust levels will rise.

[8] Higher glacial than interglacial dust levels at Vostok result primarily from a more efficient meridional atmospheric transport [*Petit et al.*, 1999]. However, more arid conditions as evidenced by glacial loess deposits contribute to increase aerosol loads. Hence glacial dust in Antarctica likely results from the conjugated effects of the expansion of arid regions and wind reinforcement. In contrast, humid conditions promote vegetation growth and thus the production of *n*-alkanes. Therefore, even though stronger glacial winds likely contributed to increase glacial *n*-alkanes to higher levels than Holocene ones, their supply to marine sediments during the last glacial period was likely modulated by changes of the vegetation biomass, and thus by the amount of rainfall in vegetation source regions.

3.2. South Africa Paleorecords

[9] It is now well established that loess soil in Patagonia is a major source of dust to Antarctica ice cores, Vostok, Dome C [*Grousset et al.*, 1992; *Basile et al.*, 1997] and EPICA Dome C [*Smith et al.*, 2003; *Delmonte et al.*, 2004]. However, Patagonia is an unlikely source of terrestrial organic carbon because of the absence or poor vegetation cover in loess areas. Terrestrial ecosystems from South Africa are more conceivable and closer sources for terrestrial *n*-alkanes to our core site.

[10] Today, the far biggest part of South Africa is grassland. The plant cover, dominated by grasses, low shrub and savannah, depends primarily on environmental factors like temperature and precipitation. In a large part of the South Africa subcontinent, known as the summer rainfall region, most of the annual rainfall originates from the Indian Ocean and occurs in summer, between October and April. Conversely, in the southern tip of the continent, the major atmospheric moisture source is the winter rainfall from the South Atlantic Ocean (Figure 1) [*Cockroft et al.*, 1987]. Mean annual precipitation in the summer region is much higher than in the winter rainfall region and is strongly influenced by tropical Indian Ocean SSTs. During warm phase of ENSO, the central Indian Ocean is generally warmer, resulting in reduced land-ocean temperature contrast and enhanced oceanic rainfall. Warmer tropical Indian SSTs are frequently associated to higher rainfall in eastern Africa during the "short rains" season of October to December [*Nicholson*, 1986] and lower rainfall in southern Africa [*Hastenrath et al.*, 1995]. This rainfall pattern is thought to have been modified during the last glacial period owing to different high-latitude boundary conditions, meridional temperature gradients and atmospheric circulation, with consequences on the vegetation.

[11] Our n-alkane record was compared to available paleorecords spanning South African climatological contrasts, where past history of vegetation and climate changes have been reconstructed. They include the modern winter rainfall region around the Cape (Cango cave stalagmite at 34°S), the summer rainfall region (stalagmites and pollens around 25°S) and Madagascar (Lake Tritrivakely, 19°47S) under the direct influence of tropical rains (Figure 1). For this comparison, we will first consider the best-documented LGM and then glacial variability on the few available continuous records over the last 27 kyr. With respect to this, speleothems are particularly pertinent archives, which provide good information on changes of temperature and rainfall. Furthermore, they generally have a good age control for comparison with other well-dated records.

[12] The first spatial reconstruction proposed by *Cockroft et al.* [1987] indicates that climate over the subcontinent was wetter and cooler from 25 to 15 ka except for the 18 to 20 ka interval where desiccation occurred, particularly at southern cape sites and eastern areas. Since, *Holmgren et al.* [2003] published a highly resolved C and O isotope data set from stalagmites in the Makapansgat Valley (24°21′S, 29°11′E, summer rain fall region, Figure 1), which represents a unique record of regional climatic change over the last 25 kyr (Figures 3a and 3b). These data also evidence drier conditions and colder temperatures by about 5.7°C, but coldest values were reached around 17 to 18 ka. A similar temperature drop of 5 to 7°C is estimated

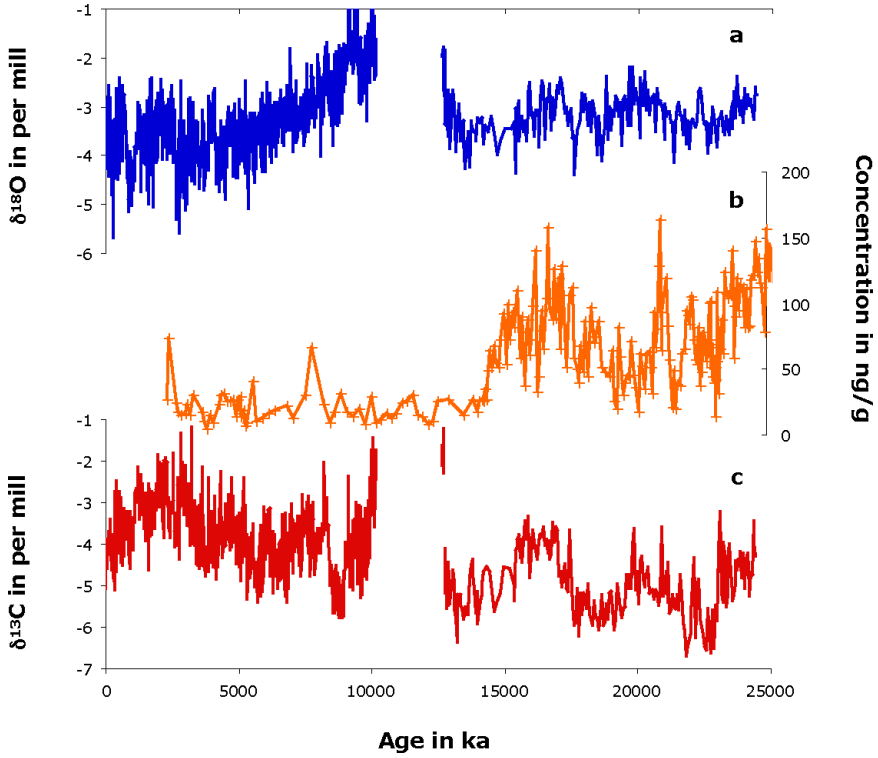

Figure 3. (a) The $\delta^{18}O$ values in Makapansgat T8 stalagmite. (b) Sum of the terrestrial *n*-alkane concentrations expressed in ng/g. (c) The $\delta^{13}C$ in the stalagmite measured in the Makapansgat T8 stalagmite over the last 24 kyr (redrawn from ftp://ftp.ncdc.noaa.gov/pub/data/paleo/speleothem/africa/cold-air-cave2003.txt).

for this period from the 30 ka oxygen isotope record of the Cango caves stalagmite (34°S; winter rainfall region, Figure 1) [*Talma and Vogel*, 1992]. These observations agree with the temperature drop across the subcontinent of 6–7°C around LGM (from 21 to 18 ka) estimated from paleoenvironmental maps of the PASH database (Paleoclimates of the Southern Hemisphere) [*Partridge et al.*, 1999]. During that time period, south of 13°S, deserts occupied the western half of the subcontinent, while the eastern part was covered by shrub land and grasses. Rainfall in the Kalahari region would have been less than 40% of the present-day rainfall [*Partridge et al.*, 1999].

[13] Limited information has been published for the period prior to LGM. The 24°S Makapansgat record indicates a progressive cooling and drying between 25 and 22 kyr B.P. After the LGM, this record shows a rapid but limited warming and wetter conditions starting ~17.5 ka and ending by a return to colder and drier climate from 15 to 13.5 ka. *Scott* [1999] reported similar findings in Wonder crater (24°26S) and Tswaing Crater (25°34S) pollen sequences with a deterioration of the temperature from 15 to 14 ka (unfortunately, no data are available between 21 and 15 ka). Drier conditions persisted between 12.7 to 10.2 ka in Makapansgat, and over a longer time interval, from 13.8 and 5 ka, in more southern Cango caves, as shown by the cessation of drip resulting in a hiatus.

[14] In summary, available data from South Africa point to cold and dry spell at the LGM, but otherwise wetter conditions between 15 and 25 ka, and a return to colder and drier climate from 15 to 14–13.5 ka. This temporal evolution contrasts with data from Lake Tritrivakely (19°47S; 46°55′E, 1778 m, Madagascar Island), more directly influenced by the tropical Indian Ocean. The latter suggests a dry period prior to LGM, from 30 ka to 22 ka, when climate is humid and colder in southern Africa, becoming cold and more humid around LGM, from 22 and 17 ka, when climate is drier and colder in southern Africa [*Williamson et al.*, 1998].

[15] Dry and cold climate in South Africa has been explained by the equatorward expansion of the circumpolar vortex, while wetter periods would be caused by its contraction and the expansion of the tropical circulation [*Holmgren et al.*, 2003]. At the LGM, maximum northward extension of the circumpolar vortex and displacement of the sub-

tropical high system over South Africa would have lowered annual precipitation and strengthened wind velocities [*Cockroft et al.*, 1987; *Tyson et al.*, 2001]. Opposite rainfall pattern at Lake Tritrivakely would result from an eastward shift of the convergence cells during dry spell conditions in southern Africa, when the polar vortex expands north [*Williamson et al.*, 1998].

3.3. Comparison of n-Alkane Record to South Africa and Marine Proxy Records

[16] The temporal evolution of terrestrial *n*-alkanes in core MD94-103 can be reconciled with the reconstructed temperature and precipitation changes in South Africa. Lower *n*-alkanes around 19–20 ka would feature reduced vegetation during drier and colder LGM climate, while increase aridity and windiness would produce higher dust deposition in EPICA ice (Figures 2c and 2d). As the subcontinent becomes wetter, *n*-alkanes progressively rise from ~19 to 20 ka till about 17 ka. At the time of Heinrich event 1 in the north (HE1), concentrations show a decline halting ~16.5 to 15 ka. Further decrease occurred after 15 ka, when climate returned drier across South Africa. Colder and wetter climate preceding the LGM is also characterized by larger inputs of terrestrial *n*-alkanes, mainly between 23 and 26 ka and during two shorter episodes centered at ~22 and 21 ka. Although less distinct, the same slight decrease as observed during HE1 seems to take place during HE2a and HE2b. Lower *n*-alkanes during cold Heinrich events of the Northern Hemisphere could be due to a decreased influence of the tropical rain in southern Africa climate.

[17] Except for the LGM, the terrestrial *n*-alkane record shares some resemblance with the $\delta^{13}C$ of Makapansgat (Figures 3b and 3c). The latter signal has been interpreted by *Holmgren et al.* [2003] as reflecting changes in the proportion of C4 (grasses) versus C3 plants. C4 grasses would be associated preferentially with the wetter summer rainfall climate, therefore lower values in the stalagmite indicate drier conditions and less grasses. While *n*-alkanes around the LGM are consistent with the dry conditions prevailing in most of southern Africa, in particular the western part, the Makapansgat stalagmite indicates that rainfall remained high, therefore suggesting that this region was not affected by subtropical anticyclones.

[18] In order to investigate the relationships between atmospheric and oceanic circulation, in particular during the Heinrich events, terrestrial biomarkers were confronted to the alkenone $U^{K'}_{37}$ index (SST_{alk}) record generated in the same core. As can be seen from Figures 2a and 2b, glacial SST_{alk} reach unexpectedly warm values (up to about 13°C). This finding has been interpreted as reflecting a strong bias caused by advection of ⟨warm⟩ "detrital" alkenones from the Agulhas Current overwhelming the local temperature signal, recorded by foraminifera (SST_{foram}) [*Sicre et al.*, 2005]. The superimposed millennial-scale apparent SST_{alk} coolings at the time of HE and around 21 ka, would result from enhanced local fluxes of cold alkenones [*Sicre et al.*, 2005]. Higher alkenone fluxes during these periods of iceberg discharge in the Northern Hemisphere has been described in subantarctic Atlantic and Pacific cores [*Sachs and Anderson*, 2005]. The co-eval warming of the upper ocean shown by SST_{foram}, also seen in the southern Pacific [*Pahnke and Zahn*, 2005], suggests enhanced ocean stratification attributable to weaker winds and/or changes in the cloud cover [*Sicre et al.*, 2005]. Either one or both factors could have promoted coccolithophorid growth. Concurrent increased ventilation of the Pacific intermediate waters (positive $\delta^{13}C$ shift of benthic foraminifera) would further support the idea of a weakening or southern shift of the westerly wind circulation [*Pahnke and Zahn*, 2005]. Finally, considering the limitations of the age models of both records, we observe a reasonably good correspondence between lower dust content in EPICA ice and cold SST_{alk} during HE, again hinting to a reduction of meridional atmospheric transport. Weakened atmospheric circulation would account for lower eolian transport, a more stratified upper-ocean and lower Ekman transport during Heinrich events.

[19] Recently, data from the western tropical Pacific [*Stott et al.*, 2002] have led to the hypothesis of super-ENSO conditions during Heinrich events implying, by analogy to modern ENSO, a weakening of tropical easterly winds. Therefore, from these results we suggest that during Northern Hemisphere Heinrich coolings, zonal winds were more sluggish (both tropical easterlies and midlatitude westerlies), transport toward the south was reduced and summer tropical rainfall was decreased over South Africa. In contrast, invigorated winds during the LGM, cold SSTs and depleted benthic $\delta^{13}C$ in the southern Pacific, would reflect enhanced Ekman transport [*Pahnke and Zahn*, 2005]. The LGM in southern Africa appears as an extreme situation of desiccation under the influence of the subtropical Atlantic anticyclone

when enhanced dust at EPICA Dome C would correspond to an expansion of the polar vortex at least in winter, as suggested earlier by [*Stuut et al.*, 2004].

4. Conclusions

[20] The comparison between continental records from South Africa and terrestrial *n*-alkanes from subantarctic Indian Ocean sediments provided an integrated picture of atmospheric circulation changes during Heinrich events and the LGM. Around 19–20 ka, the expansion of the dry atmosphere subsidence corresponding to the subtropical high pressure zone over southern Africa, as a result of a northern expansion of the polar vortex, significantly reduced moisture transfer from the tropical Indian Ocean by the easterlies, in the summer rainfall region.

[21] Apart from the LGM, the stronger influence of the glacial tropical circulation allowed wetter conditions over most of the African subcontinent. This period was characterized by several episodes (mostly coinciding with HE) of sluggish zonal winds (easterly and westerly winds) and reduced meridional transport associated with drier conditions of Tropical Africa. El Niño-like could have played a part in the reduced influence of tropical rainfall regime during Heinrich events.

Acknowledgments

[22] This work was supported by the INSU/CNRS program PNEDC (Programme National d'Etude de la Dynamique du Climat). We thank the IFRTP, IPEV, and *Marion Dufresne* officers and crew for support and organization of the coring cruise PACIMA. This is an IPSL study and LSCE contribution 1870.

References

Bard, E. (1988), Correction of accelerator mass spectrometry 14C ages measured in planktonic foraminifera: Paleoceanographic implications, *Paleoceanography*, *3*, 635–645.

Basile, I., F. E. Grousset, M. Revel, J. R. Petit, P. E. Biscaye, and N. I. Barkov (1997), Patagonian origin of glacial dust deposited in East Antarctica (Vostok and Dome C) during glacial stages 2, 4 and 6, *Earth Planet. Sci. Lett.*, *146*, 573–589.

Charles, C. D., J. Lynch-Stieglitz, U. S. Ninnemann, and R. G. Fairbanks (1996), Climate connections between the hemisphere revealed by deep sea sediment core/ice core correlations, *Earth Planet. Sci. Lett.*, *142*, 19–27.

Cockroft, M. J., M. J. Wilkinson, and P. D. Tyson (1987), The application of a present-day climatic model to the late Quaternary in southern Africa, *Clim. Change*, *10*, 161–181.

Conte, M. H., and J. C. Weber (2002), Plant biomarkers in aerosols record isotopic discrimination of terrestrial photosynthesis, *Nature*, *417*, 639–641.

Crosta, X., A. Sturm, L. Armand, and J.-J. Pichon (2004), Late Quaternary Sea ice history in the Indian sector of the Southern Ocean as recorded by diatom assemblages, *Mar. Micropaleontol.*, *50*, 209–223.

Delmonte, B., I. Basile-Doelsch, J.-R. Petit, V. Maggi, M. Revel-Rolland, A. Michard, E. Jagoutz, and F. Grousset (2004), Comparing the EPICA and Vostok dust records during the last 220,000 years: Stratigraphical correlation and provenance in glacial periods, *Earth Sci. Rev.*, *66*, 63–87.

EPICA Community Members (2004), Eight glacial cycles from an Antarctic ice core, *Nature*, *429*, 623–628.

Gagosian, R. B., and E. T. Peltzer (1987), The importance of atmospheric input of terrestrial organic matter to deep sea sediments, *Org. Geochem.*, *10*, 661–669.

Grousset, F. E., P. E. Biscaye, M. Revel, J. R. Petit, K. Pye, S. Joussaume, and J. Jouzel (1992), Antarctic (Dome C) ice-core dust at 18 k.y. B.P.: Isotopic constraints on origin, *Earth Planet. Sci. Lett.*, *111*, 175–182.

Hastenrath, S., L. Greischar, and J. van Heerden (1995), Prediction of the summer rainfall over South Africa, *J. Clim.*, *8*, 1511–1518.

Holmgren, H., J. A. Lee-Thorp, G. R. J. Cooper, K. Lundblad, T. C. Partridge, L. Scott, R. Sithaldeen, A. S. Talma, and P. D. Tyson (2003), Persistent millennial-scale climatic variability over the past 25,200 years in southern Africa, *Quat. Sci. Rev.*, *22*, 2311–2326.

Huang, Y., F. A. Street-Perrot, S. E. Metcalfe, M. Brenner, M. Moreland, and K. H. Freeman (2001), Climate change as the dominant control on glacial/interglacial variations in C_3 and C_4 plant abundance, *Science*, *293*, 1647–1651.

Hughen, K. A., T. I. Eglinton, L. Xu, and M. Makou (2004), Abrupt tropical response to rapid climate changes, *Science*, *304*, 1955–1959.

Kaiser, J., F. Lamy, and D. Hebbeln (2005), A 70-kyr sea surface temperature record off southern Chile (Ocean Drilling Program Site 1233), *Paleoceanography*, *20*, PA4009, doi:10.1029/2005PA001146.

Lamy, F., J. Kaiser, U. Ninnemann, D. Hebbeln, H. W. Arz, and J. Stoner (2004), Antarctic timing of the surface water changes off Chile and Patagonian ice sheet response, *Science*, *304*, 1959–1962.

Mazaud, A., M.-A. Sicre, U. Ezat, J.-J. Pichon, J. Duprat, C. Laj, C. Kissel, L. Beaufort, E. Michel, and J.-L. Turon (2002), Geomagnetic-assisted stratigraphy and sea surface temperature changes in core MD94–103 (southern Indian Ocean): Possible implications for north-south climatic relationships around H4, *Earth Planet. Sci. Lett.*, *201*, 159–170.

Nicholson, S. E. (1986), The spatial coherence of African rainfall anomalies: Interhemispheric teleconnections, *J. Clim. Appl. Meteorol.*, *25*, 1365–1381.

Pahnke, K., and R. Zahn (2005), Southern Hemisphere water mass conversion linked with North Atlantic climate variability, *Science*, *307*, 1741–1745.

Partridge, T. C., L. Scott, and J. E. Hamilton (1999), Synthetic reconstructions of southern African environments during the Last Glacial Maximum (21–18 kyrs) and the Holocene Altithermal (8–6 kyrs), *Quat. Int.*, *57/58*, 207–214.

Petit, J. R., et al. (1999), Climate and atmospheric history of the past 420,000 years from the Vostok ice core, Antarctica, *Nature*, *399*, 429–436.

Prahl, F. G., L. A. Muehlhausen, and D. L. Zahnle (1988), Further evaluation of long-chain alkenones as indicators of

paleoceanographic conditions, *Geochim. Cosmochim. Acta*, *52*, 2303–2310.

Quartly, G. D., and M. A. Srokosz (1993), Seasonal variations in the region of the Agulhas Retroflection: Studies with Geosat and FRAM, *J. Phys. Oceanogr.*, *23*, 2107–2124.

Rintoul, S. R., C. Hughes, and D. Olbers (2001), *The Antarctic Circumpolar Current System: Ocean Circulation and Climate*, edited by G. Sieder, J. Church, and J. Gould, Elsevier, New York.

Sachs, J. P., and R. F. Anderson (2003), Fidelity of alkenone paleotemperatures in southern Cape Basin sediment drifts, *Paleoceanography*, *18*(4), 1082, doi:10.1029/2002PA000862.

Sachs, J. P., and R. F. Anderson (2005), Increased productivity in the subantarctic ocean during Heinrich events, *Nature*, *434*, 1118–1121.

Sachs, J. P., R. F. Anderson, and S. J. Lehman (2001), Glacial surface temperatures of the southeast Atlantic Ocean, *Science*, *293*, 2077–2079.

Saji, N. H., B. N. Goswami, P. N. Vinayachandran, and T. Yamagata (1999), A dipole mode in the tropical Indian Ocean, *Nature*, *401*, 360–363.

Scott, L. (1999), The vegetation history and climate in the Savanna Biome, South Africa since 190,000 ka: A comparison of pollen data from Tswaing Crater (the Pretoria Saltpan) and Wonderkrater, *Quat. Int.*, *57*, 215–223.

Sicre, M.-A., and E. T. Peltzer (2004), Lipid geochemistry of remote aerosols from the southwestern Pacific Ocean sector, *Atmos. Environ.*, *38*(11), 1615–1624.

Sicre, M.-A., J.-C. Marty, A. Saliot, X. Aparicio, J. Grimalt, and J. Albaiges (1987), Aliphatic and aromatic hydrocarbons in different sized aerosols over the Mediterranean Sea: Occurrence and origin, *Atmos. Environ.*, *10*, 2247–2259.

Sicre, M.-A., L. Labeyrie, U. Ezat, J. Duprat, J.-L. Turon, E. Michel, S. Schmidt, and A. Mazaud (2005), Southern Indian Ocean response to Northern Hemisphere Heinrich events, *Earth Planet. Sci. Lett.*, *240*(3–4), 724–731, doi:10.1016/j.epsl2005.09.032.

Smith, J., D. Vance, R. A. Kemp, C. Archer, P. Toms, M. King, and M. Zarate (2003), Isotopic constraints on the source of Argentinean loess—With implications for atmospheric circulation and the provenance of Antarctic dust during recent glacial maxima, *Earth Planet. Sci. Lett.*, *212*, 181–196.

Stott, L., C. Poulsen, S. Lund, and R. Thunnell (2002), Super ENSO and global climate oscillations at millennial time scales, *Science*, *297*, 222–226.

Stuut, J.-B. W., X. Crosta, K. van der Borg, and R. Schneider (2004), Relationship between Antarctic sea ice and southwest Africa climate during the late Quaternary, *Geology*, *32*, 909–912.

Talma, A. S., and J. C. Vogel (1992), Late Quaternary paleotemperatures derived from a speleothem from Cango Caves, Cape Province, South Africa, *Quat. Res.*, *37*, 203–213.

Ternois, Y., M.-A. Sicre, A. Boireau, M. H. Conte, and G. Eglinton (1997), Evaluation of long-chain alkenones as paleo-temperature indicators in the Mediterranean Sea, *Deep Sea Res., Part I*, *44*, 271–286.

Ternois, Y., M. Sicre, and M. Paterne (2000), Climatic changes along the northwestern African continental margin over the last 30 kyrs, *Geophys. Res. Lett.*, *27*(1), 133–136.

Tyson, P. D., E. O. Odada, and T. C. Partridge (2001), Late Quaternary environmental change in southern Africa, *S. Afr. J. Sci.*, *97*, 139–150.

Webster, P. J., A. M. Moore, J. P. Loschnigg, and R. R. Leben (1999), Coupled ocean-atmosphere dynamics in the Indian Ocean during 1997–1998, *Nature*, *401*, 356–360.

Williamson, D., A. Jelinowska, C. Kissel, P. Tucholka, E. Gibert, F. Gasse, M. Massault, M. Taieb, E. van Campo, and K. Wieckowski (1998), Mineral-magnetic proxies of erosion/oxidation cycles in tropical maar-lake sediments (Lake Tritrivakely, Madagascar): Paleoenvironmental implications, *Earth Planet. Sci. Lett.*, *155*, 205–219.